Three-Coordinated Boron-11 Chemical Shifts in Borates

Scott Kroeker* and Jonathan F. Stebbins

Department of Geological and Environmental Sciences, Stanford University, Stanford, California 94305-2115

Received March 20, 2001

Despite the importance of ^{11}B nuclear magnetic resonance (NMR) in structural studies of borate glasses, no clear means of correlating NMR parameters with the number of nonbridging oxygens on three-coordinate boron has been demonstrated. In this work, a series of anhydrous, polycrystalline, binary borates has been examined by ^{11}B magic-angle spinning (MAS) NMR to obtain precise measurements of their three-coordinate boron isotropic chemical shifts. The shifts generally increase with the replacement of bridging oxygens by nonbridging oxygens, ranging from 14.6 ppm in crystalline B_2O_3 to 22.5 ppm in magnesium orthoborate. The underlying physical basis for this trend is satisfactorily accounted for by considering second neighbor effects using bond valence sums. These data are supportive of a structural model for B_2O_3 glass in which 72% of the boron atoms are in rings. High-field MAS NMR experiments (B_0 = 18.8 T) indicate that the boron shielding is anisotropic, with greater anisotropy measured for three-coordinate borons possessing one or two nonbridging oxygens, than for those with zero or three nonbridging oxygens.

Introduction

The structure and properties of borate glasses have been studied since the 19th century.[1] Extensive research supports mature industrial sectors ranging from durable cookware to optical components to "fiberglass" composites.[2] And yet, fundamental structural questions remain. One issue key to borate glass stability and miscibility in multicomponent systems is the role of superstructural units such as planar rings in network formation. Amorphous borates generally consist of a network of interconnected three- and four-coordinated boron−oxygen units (Scheme 1), charge balanced by network modifying cations. If all three oxygens are bridging high field-strength cations (e.g., B, Si, P, Al), the $BO_{3/2}$ species are said to be fully polymerized, with a high degree of network connectivity. The extent to which such species form three-membered planar "boroxol" rings in pure B_2O_3 and low alkali glasses is a question of long-standing debate. Negatively charged four-coordinated tetrahedral $BO_{4/2}$ units are found in glass compositions with low concentrations of alkali or alkaline earth oxides. At higher alkali loadings, bridging oxygens on the trigonal planar borons are converted to nonbridging oxygens, bonded to only one boron and possessing a partial negative charge counterbalanced by one or more network modifiers (e.g., Na, Cs, Mg, Ba). At still higher loadings, two and three bridging oxygens may become nonbridging, effectively breaking down the borate network. This depolymerization may be denoted by the T^n nomenclature, where T stands for "ternary" (by analogy to the widespread Q^n nomenclature for quaternary silicon), and the superscript n = 0−3 indicates the number of bridging oxygens. Thus, T^3 indicates a high degree of network connectivity, and T^0 indicates extensive depolymerization.

Scheme 1. Schematic Depiction of the Various Borate Species Discussed in This Paper[a]

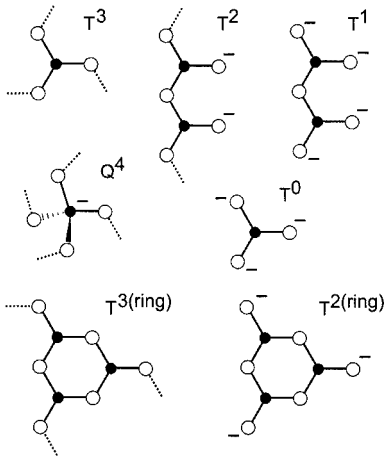

[a] Solid dots represent boron, and open circles represent oxygen. Dotted lines indicate bonding to other network cations; negative signs indicate nonbridging oxygens on three-coordinate boron.

Nuclear magnetic resonance (NMR) has played a prominent role in the study of borate glasses, dating back to 1958 when Silver and Bray published ^{11}B wide-line NMR spectra of several model and commercial borate glasses.[3] Many of the structural models for borate, borosilicate, and aluminoborate glasses were developed on the basis of ^{11}B NMR data.[4] Boron-11 is 80% abundant naturally and exhibits high sensitivity in NMR experiments. A spin-3/2 nuclide, it possesses a quadrupole moment (eQ) which couples with the local electric field gradient (eq) tensor to yield anisotropic peak shapes which can be

* To whom correspondence should be addressed. Current address: University of Manitoba, Department of Chemistry, 350 Parker Building, Winnipeg, MB, R3T 2N2, Canada. E-mail: Scott_Kroeker@UManitoba.ca. Phone: 204-474-9335. Fax: 204-474-7608.

(1) Smith, R. A. In *Borate Glasses, Crystals and Melts*; Wright, A. C., Feller, S. A., Hannon, A. C., Eds.; Society of Glass Technology: Sheffield, UK, 1997; pp 313−322.
(2) Cable, M., Parker, J. M., Eds. *High-Performance Glasses*; Chapman and Hall: New York, 1992.
(3) Silver, A. H.; Bray, P. J. *J. Chem. Phys.* **1958**, *29*, 984−990.
(4) Bray, P. J. *Inorg. Chim. Acta* **1999**, *289*, 158−173.

10.1021/ic010305u CCC: $20.00
Published on Web 10/04/2001

characterized in terms of a quadrupole coupling constant, $C_Q = (eQ)(eq)/h$, and an asymmetry parameter, η, describing the relative magnitudes of the tensor components.[4] Early NMR work on borates was performed on nonspinning samples at very low magnetic fields ($B_0 < 1$ T). Although no chemical shift information was available from such spectra, the central ($+^1/_2$, $-^1/_2$) transition (CT) could be observed and the quadrupolar parameters readily assessed. Once it was discovered that the four-coordinated boron possesses a small C_Q (<1 MHz), whereas the three-coordinated boron has a much larger C_Q (2.4−2.9 MHz), the corresponding difference in peak breadth could be exploited to deconvolve the signals and obtain the relative population of these species. Distinguishing between different types of three-coordinate borons, however, is more difficult. Whereas the asymmetry parameter is small ($\eta < 0.3$) for T^3 and T^0 groups and larger ($0.5 \leq \eta \leq 0.8$) for T^1 and T^2 groups, the C_Q values provide no such systematics from which reliable speciation may be derived.[5]

With modern high-field magic-angle spinning (MAS) NMR, broadening due to the quadrupolar interaction is significantly reduced, and complete resolution of three- and four-coordinated boron is achieved at fields above 11.7 T (500 MHz ^{1}H frequency) by virtue of greater intrinsic chemical shift dispersion. The precision with which the isotropic chemical shift δ_{iso} for the sharp $BO_{4/2}$ resonance may be measured by ^{11}B MAS NMR of glasses has facilitated systematic studies of structural influences on this parameter.[6−8] Each bonded three-coordinate boron group appears to increase $\delta_{iso}(BO_{4/2})$ by about 0.5 ppm, while a linkage to tetrahedral silicon induces a 0.5 ppm decrease in the shift.[6] Parallel attempts to rationalize three-coordinate boron peak positions in glasses with respect to structure have been less successful in these same studies. Boron-11 MAS NMR of a series of crystalline binary borates uncovered no discernible trend in δ_{iso} for three-coordinated boron with different numbers of nonbridging oxygens.[9] By analogy with the tetrahedral boron shifts, some authors have postulated the presence of borosiloxane linkages based on highly shielded peaks (smaller chemical shifts) in sol−gel produced borosilicate glasses,[10,11] but little direct evidence has been presented. Some insight into the chemical shifts of three-coordinated boron has been garnered using dynamic-angle spinning (DAS) NMR of crystalline and glassy potassium borates.[12,13] These works contrast the DAS NMR spectral characteristics of ring and nonring borons. They report subtle differences among the various types of rings containing T^3 and T^2 units, all with DAS peaks centered approximately 3−5 ppm to higher frequency of the nonring T^3 in potassium diborate. Finally, high-field MAS NMR is capable of detecting spinning sidebands (ssbs) arising from the ^{11}B ($\pm^3/_2$, $\pm^1/_2$) satellite transitions (STs). As these peak shapes and positions depend differently on the chemical shift and quadrupolar interactions than does the central transition, enhanced resolution of boron sites may be realized.[14,15] By this approach, Jäger et al. reported three distinct three-coordinate boron sites in a sodium borosilicate glass having chemical shifts ranging over 4 ppm.[16]

Despite these efforts, more work is needed to fully understand how ^{11}B shielding is related to local structure. In this study, a series of polycrystalline binary borates are examined by high-field ($B_0 = 14.1$ T) ^{11}B MAS NMR to obtain precise values of δ_{iso} corresponding to all degrees of three-coordinate boron connectivity, T^n ($n = 0-3$). Central and satellite transitions are analyzed to enhance confidence in the measured chemical shifts and quadrupolar parameters. Selected compounds are also investigated at 18.8 T (800 MHz ^{1}H frequency) to assess the effects of anisotropic chemical shielding.

Experimental Section

Crystalline B_2O_3, prepared according to the literature,[17] was kindly provided by Dr. R. A. Smith (U. S. Borax). Cesium enneaborate ($Cs_2O\cdot 9B_2O_3$ = Cs9B) was prepared by fusing appropriate amounts of Cs_2CO_3 and boric acid.[18] The dehydrated and decarbonated melt was supercooled to just below its liquidus temperature[19] of 596 °C for 24 h and seeded with 2 wt % TiO_2 to facilitate crystallization. The calcium and lithium metaborates ($CaO\cdot B_2O_3$ = CaB; $Li_2O\cdot B_2O_3$ = LiB) were obtained from commercial sources: Alfa Aesar and Southwestern Analytical Chemicals, Inc., respectively. The latter was melted and recrystallized to obtain the pure LiB phase. Anomalous ^{11}B MAS NMR line shapes revealed that the long, needlelike lithium metaborate crystals packed into the MAS NMR rotor with a preferred crystallite orientation, despite extensive grinding with mortar and pestle. To produce a random orientational distribution, this sample was fixed in epoxy resin and ground with abrasive paper. Sodium metaborate ($Na_2O\cdot B_2O_3$ = NaB) and sodium pyroborate ($2Na_2O\cdot B_2O_3$ = 2NaB) were crystallized from the melts as previously described.[20,21] In the preparation of magnesium pyroborate ($2MgO\cdot B_2O_3$ = 2MgB), a mixture of "magnesium carbonate" ($4MgCO_3\cdot Mg(OH)_2\cdot nH_2O$) and amorphous B_2O_3 was dehydrated and decarbonated by slow heating to 400 °C. The reagent mixture was then held at 950 °C for 12 h, at 1200 °C for 24 h and annealed at 1000 °C for 24 h according to the synthetic procedure described by Guo et al.[22] X-ray diffraction of the resulting white, crystalline powder indicated that the desired triclinic pyroborate phase was obtained,[23] in addition to a second, minor phase (<10%) identified as magnesium orthoborate ($3MgO\cdot B_2O_3$ = 3MgB).[24] Lanthanum orthoborate ($La_2O_3\cdot B_2O_3$ = LaB) was synthesized by mixing an excess of B_2O_3 glass (molar ratio, 0.65) with dry La_2O_3 powder and holding for 1 h at 1500 °C. After three cycles of cooling and reannealing, the weight lost due to B_2O_3 evaporation at this high temperature yielded a calculated 1:1 molar ratio. X-ray diffraction indicated the presence of the desired orthorhombic product,[25] as well as a contribution from a high-temperature

(5) Kriz, H. M.; Bray, P. J. *J. Magn. Reson.* **1971**, *4*, 76−84.
(6) van Wüllen, L.; Müller-Warmuth, W.; Papageorgiou, D.; Pentinghaus, H. J. *J. Non-Cryst. Solids* **1994**, *171*, 53−67.
(7) Müller-Warmuth, W. *Z. Naturforsch., A: Phys. Sci.* **1995**, *51a*, 585−590.
(8) Martens, R.; Müller-Warmuth, W. *J. Non-Cryst. Solids* **2000**, *264*, 167−175.
(9) Müller, D.; Grimmer, A. R.; Timper, U.; Heller, G.; Shakibaie-Moghadam, M. *Z. Anorg. Allg. Chem.* **1993**, *619*, 1262−1268.
(10) Irwin, A. D.; Holmgren, J. S.; Jonas, J. *J. Non-Cryst. Solids* **1988**, *101*, 249−254.
(11) Sorarù, G. D.; Dallabona, N.; Gervais, C.; Babonneau, F. *Chem. Mater.* **1999**, *11*, 910−919.
(12) Youngman, R. E.; Zwanziger, J. W. *J. Non-Cryst. Solids* **1994**, *168*, 293−297.
(13) Youngman, R. E.; Zwanziger, J. W. *J. Phys. Chem.* **1996**, *100*, 16720−16728.
(14) van Wüllen, L.; Müller-Warmuth, W. *Solid State Nucl. Magn. Reson.* **1993**, *2*, 279−284.
(15) Kunath-Fandrei, G.; Ehrt, D.; Jäger, C. *Z. Naturforsch., A: Phys. Sci.* **1995**, *50a*, 413−422.
(16) Jäger, C.; Herzog, K.; Thomas, B.; Feike, M.; Kunath-Fandrei, G. *Solid State Nucl. Magn. Reson.* **1995**, *5*, 51−61.
(17) Kline, D.; Bray, P. J.; Kriz, H. M. *J. Chem. Phys.* **1968**, *48*, 5277−5278.
(18) Krogh-Moe, J. *Acta Crystallogr.* **1967**, *23*, 427−430.
(19) Reser, M. K.; Ed. *Phase Diagrams for Ceramists*; The American Ceramic Society: Columbus, Ohio, 1964.
(20) George, A. M.; Sen, S.; Stebbins, J. F. *Solid State Nucl. Magn. Reson.* **1997**, *10*, 9−17.
(21) Stebbins, J. F.; Zhao, P.; Kroeker, S. *Solid State Nucl. Magn. Reson.* **2000**, *16*, 9−19.
(22) Guo, G.; Cheng, W.; Chen, J.; Huang, J.; Zhang, Q. *Acta Crystallogr.* **1995**, *C51*, 351−352.
(23) Block, S.; Burley, G.; Perloff, A.; R. D. Mason, J. *J. Res. Natl. Bur. Stand. (U.S.)* **1959**, *62*, 95−100.
(24) Berger, S. V. *Acta Chem. Scand.* **1949**, *3*, 660−675.
(25) Abdullaev, G. K.; Dzafarov, G. G.; Mamedov, K. S. *Azerb. Khim. Z.* **1976**, *3*, 117−120.

$LaBO_3$ polymorph, the crystal structure of which remains undetermined.[26] Boron-11 MAS NMR confirmed the presence of two components. This mixture was ground and reannealed at 1450 °C to isolate the orthorhombic material. Crystallinity was verified in all cases by visual inspection at 400× magnification with a polarizing microscope. The identities of all samples (except CaB) were confirmed by powder X-ray diffraction. All compounds were dried to a constant mass at 250 °C prior to NMR analysis and stored in a desiccator over phosphorus pentoxide.

Boron-11 NMR spectra were acquired at 192.4 MHz ($B_0 = 14.1$ T) and 256.4 MHz ($B_0 = 18.8$ T) on Varian Inova spectrometers. Samples ranging in mass from 10 to 70 mg were packed into 3.2 mm o.d. rotors and spun at the magic angle with rates of 12 to 20 kHz. Short radio frequency pulses (~0.2 μs) were chosen not to exceed one-sixth the "solution 90°" pulse duration,[27] as calibrated using a 0.1 M aqueous solution of boric acid. A typical experiment involved the acquisition of 4K data points, sampled in 2−5 μs intervals. This data table was zero-filled to 8K points and multiplied by an exponential function corresponding to 10 Hz line broadening before Fourier transformation. The number of transients averaged to produce a given spectrum ranged from 256 to 1024, with relaxation delays of 1−60 s. Frequencies are reported with respect to neat $F_3B{\cdot}O(CH_2CH_3)_2$, which resonates at −19.6 ppm relative to that observed for 0.1 M boric acid (aq).[28]

Line shape modeling was carried out using the Varian program, STARS. In fitting the satellite transition spinning sideband line shapes, it was necessary to account for small (<0.05°) deviations from the magic angle. Uncertainties in the cited parameters were estimated by visual inspection of the agreement between calculated and experimental spectra.

Results

Boron-11 MAS NMR spectra of selected crystalline borates recorded at 192.4 MHz ($B_0 = 14.1$ T) are presented in Figures 1−5, along with the line shapes calculated by the parameters listed in Table 1.

The observed ^{11}B MAS NMR central transition line shape of B_2O_3 can be calculated with $\delta_{iso} = 14.6 \pm 0.1$ ppm, $C_Q = 2.69 \pm 0.01$ MHz, and a small quadrupolar asymmetry, $\eta < 0.05$ (Figure 1a). The chemical shift agrees with a recent measurement by Joo et al.[29] A calculation of the satellite transition spinning sideband manifold confirms the C_Q, while providing an asymmetry parameter of 0.05 to 0.07. The ^{11}B NMR spectrum of the nonspinning sample (not shown) reveals two singularities for each satellite transition, confirming that the quadrupolar tensor is nearly, but not exactly, axially symmetric. The separation between these features gives a value of $\eta = 0.035 \pm 0.005$, and the difference between their average values yields $C_Q = 2.70$ MHz. These values are similar to those derived from two independent measurements by ^{11}B wide-line NMR at $B_0 \approx 1$ T, $C_Q = 2.76 \pm 0.03$ MHz.[17,30] A zero-field nuclear quadrupole resonance (NQR) study of this material,[31] obtained $C_Q = 2.703$ MHz at 77 K, while a detailed analysis of weak ^{10}B peaks enabled the authors to obtain even more precise ^{11}B quadrupole parameters: $C_Q = 2.70110 \pm 0.00016$ MHz and $\eta = 0.06687 \pm 0.00036$. At 300 K, a combined NMR and NQR effort determined the quadrupole coupling constant to be slightly smaller: $C_Q = 2.6826 \pm 0.0005$ MHz.[4]

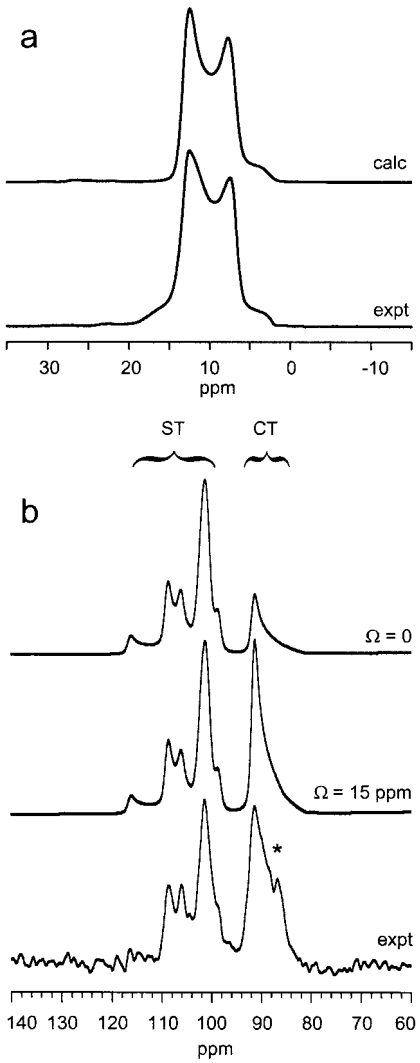

Figure 1. Experimental and calculated ^{11}B MAS NMR spectra of crystalline B_2O_3 at 14.1 T: (a) centerband; (b) first-order spinning sideband possessing both central and satellite transition contributions, calculated with isotropic and anisotropic chemical shielding. Impurity phase marked with an asterisk.

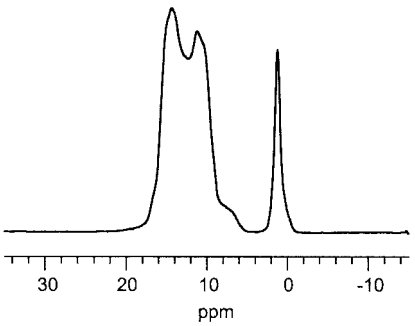

Figure 2. ^{11}B MAS NMR spectrum of Cs9B collected at 14.1 T, depicting 3- and 4-fold coordinated boron peaks.

Anisotropic chemical shielding is required to more accurately fit the MAS NMR spectrum at 14.1 T (Figure 1b). A convenient description of nuclear magnetic shielding in terms of the observable chemical shift principal components, $\delta_{11} \geq \delta_{22} \geq \delta_{33}$, is by the full extent of the shielding *span*, $\Omega = \delta_{11} - \delta_{33}$, and by the *skew*, $\kappa = 3(\delta_{22} - \delta_{iso})/\Omega$, indicating the relative positioning of the components with respect to each other.[32]

(26) Levin, E. M.; Robbins, C. R.; Waring, J. L. *J. Am. Ceram. Soc.* **1961**, *44*, 87−91.
(27) Samoson, A.; Lippmaa, E. *Phys. Rev. B: Condens. Matter* **1983**, *28*, 6567−6570.
(28) Dewar, M. J. S.; Jones, R. *J. Am. Chem. Soc.* **1967**, *89*, 2408−2410.
(29) Joo, C.; Werner-Zwanziger, U.; Zwanziger, J. W. *Solid State Nucl. Magn. Reson.* **2000**, *16*, 77−83.
(30) Svanson, S. E.; Johansson, R. *Acta Chem. Scand.* **1969**, *23*, 628−634.
(31) Gravina, S. J.; Bray, P. J.; Petersen, G. L. *J. Non-Cryst. Solids* **1990**, *123*, 165−169.
(32) Mason, J. *Solid State Nucl. Magn. Reson.* **1993**, *2*, 285−288.

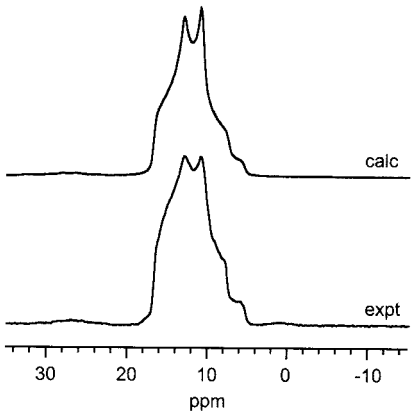

Figure 3. ^{11}B MAS NMR spectrum of CaB central transition at 14.1 T with calculation. Disparity between experimental and calculated intensities is due to a nonrandom crystallite orientational distribution.

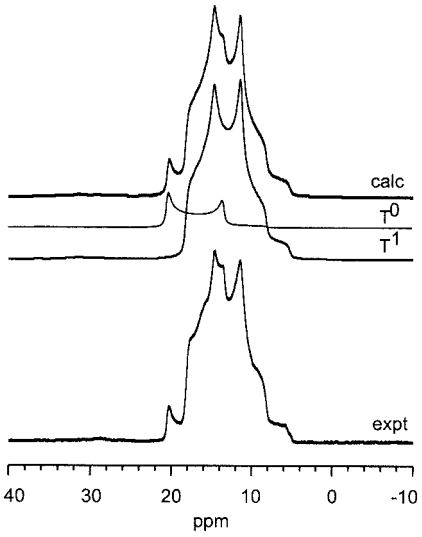

Figure 4. ^{11}B MAS NMR spectrum of 2MgB (T^1) and minor phase 3MgB (T^0) at 14.1 T, with total peakshape calculation and individual components.

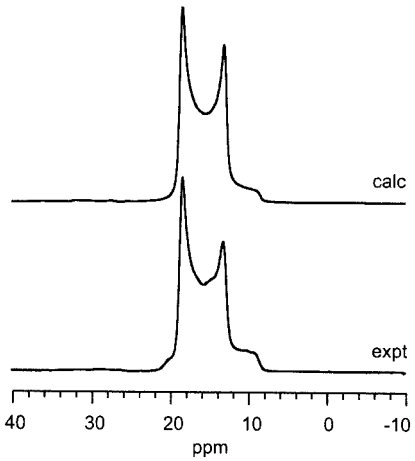

Figure 5. ^{11}B MAS NMR spectrum of LaB central transition at 14.1 T with calculation.

Assuming that the shielding tensor principal components are aligned with the principal components of the corresponding quadrupolar interaction tensor (see Discussion), the intensities of the first- and second-order CT ssbs can be modeled with a shielding anisotropy characterized either by $\Omega = 15$ ppm and $\kappa = +1$, or by a larger span of 60 ppm, with a negative skew, $\kappa = -1$. The ^{11}B NMR spectrum of the stationary sample is not useful in discriminating between these possibilities due to homonuclear dipolar broadening which obscures the characteristic features of the CT line shape. At a higher magnetic field, however, the shielding interaction becomes more prominent, and the quadrupolar interaction less so, thus providing a means of resolving this ambiguity. The ^{11}B MAS NMR spectrum (all transitions) acquired at 18.8 T (not shown) can be successfully modeled only with a shielding tensor of $\kappa = +1$ and $\Omega = 15$ ppm.

The ^{11}B MAS NMR centerband of cesium enneaborate at 14.1 T is presented in Figure 2. This compound contains several crystallographically inequivalent trigonal boron sites,[18] all of which appear to have similar, though not identical, NMR properties. As such, the broad signal representing a superposition of T^3 resonances exhibits too few features at this field to enable an unambiguous determination of individual site parameters. However, considering only the low-frequency edge of the central transition band, and making the reasonable assumption that C_Q is not smaller than 2.45 MHz ($\eta < 0.3$),[5] then δ_{iso} must exceed 16.4 ppm for all T^3 components. On the other hand, treating the full width of the pattern as though it were from a single site, C_Q cannot exceed 2.6 MHz. In this limiting case, δ_{iso} must be less than 17.2 ppm for all the T^3 sites. Thus, accepting some constraints on C_Q and η from the literature, δ_{iso} for these three-coordinated boron components lie in the range of 16.4 to 17.2 ppm. The four-coordinate boron has $\delta_{iso} = +0.95$ ppm, with a C_Q estimated from the ST ssbs of 200 ± 50 kHz and $\eta > 0.5$. Greater overlap among the T^3 sites in Cs9B is present in the MAS NMR spectrum at 18.8 T (not shown). A single set of parameters can be obtained in this case by carefully fitting the intensities and line shapes of the first several spinning sidebands of all transitions. Possible C_Q values are < 2.55 MHz, constraining δ_{iso} to 16.7 ± 0.2 ppm. The chemical shielding anisotropy, established from 14.1 and 18.8 T data as for crystalline B_2O_3, spans 21 ± 2 ppm, with $\kappa = +1$.

The ^{11}B NMR parameters for calcium metaborate (Figure 3), lithium metaborate, magnesium pyroborate/orthoborate (Figure 4) and lanthanum orthoborate (Figure 5) were obtained from line shape simulations of the central transitions; quadrupolar parameters were verified by measuring the separation of the satellite and central transition centers of gravity.[33,34] Calcium metaborate was studied by ^{11}B NMR in 1968,[35] and was the first observation of the large quadrupolar asymmetry parameter for three-coordinate boron containing one nonbridging oxygen, with $C_Q = 2.58 \pm 0.02$ MHz and $\eta = 0.55 \pm 0.01$. Using ^{11}B and ^{10}B NQR spectroscopy at 77 K, Mao and Bray found $C_Q = 2.5943 \pm 0.0005$ MHz and $\eta = 0.515 \pm 0.001$, while a combination of ^{11}B NQR and NMR at 300 K yielded $C_Q = 2.5735 \pm 0.0005$ MHz and $\eta = 0.511 \pm 0.002$.[36] The current results from ^{11}B MAS NMR are close to those reported previously. As in the present work, the lithium metaborate sample in ref 5 was impure, with the X-ray diffraction peaks not assignable to any known crystalline lithium borates. Line shape analysis of the wide-line NMR data yielded $C_Q = 2.58 \pm 0.03$ MHz and $\eta = 0.55 \pm 0.02$. Despite spectral overlap with an additional phase, increasing the error margin in both studies, the data are in reasonable agreement. The present ^{11}B

(33) Jäger, C. In *NMR Basic Principles and Progress*; Blümich, B., Ed.; Springer-Verlag: New York, 1994; Vol. 31, pp 133−170.
(34) Samoson, A. *Chem. Phys. Lett.* **1985**, *119*, 29−32.
(35) Kriz, H. M.; Bishop, S. G.; Bray, P. J. *J. Chem. Phys.* **1968**, *49*, 557−561.
(36) Mao, D.; Bray, P. J. *Solid State Nucl. Magn. Reson.* **1992**, *1*, 255−260.

Table 1. ^{11}B NMR Parameters, Structure Type, and References for Crystalline Borates[a]

	δ_{iso} (ppm)	C_Q (MHz)	η	Ω (ppm)	T^n	ref(s)
B_2O_3	14.6 ± 0.1	2.690 ± 0.005	<0.05	15 ± 2	T^3	40−42
$Cs_2O{\cdot}9B_2O_3$	16.7 ± 0.2	2.50 ± 0.05	(0.2)	21 ± 2	T^3(ring)	18
$Li_2O{\cdot}B_2O_3$	17.08 ± 0.06	2.56 ± 0.01	0.60 ± 0.03	n.d.	T^2	44
$CaO{\cdot}B_2O_3$	17.15 ± 0.05	2.53 ± 0.01	0.63 ± 0.02	38 ± 5	T^2	43
$K_2O{\cdot}B_2O_3$	18.1[b]	(2.41)	(0.8)	n.d.	T^2(ring)	65,66
$Na_2O{\cdot}B_2O_3$	18.2 ± 0.3	2.41 ± 0.02	0.8 ± 0.05	n.d.	T^2(ring)	45,93
$2MgO{\cdot}B_2O_3$	18.7 ± 0.1	2.78 ± 0.02	0.48 ± 0.02	33 ± 5	T^1	22,23
$2Na_2O{\cdot}B_2O_3$	21.8 ± 0.2	2.63 ± 0.02	0.50 ± 0.04	n.d.	T^1	47
$La_2O_3{\cdot}B_2O_3$	20.4 ± 0.1	2.67 ± 0.01	0.05 ± 0.05	17 ± 2	T^0	25
$3MgO{\cdot}B_2O_3$	22.5 ± 0.1	2.94 ± 0.02	<0.05	n.d.	T^0	24

[a] Values in parentheses were fixed in the calculations. Values not determined indicated by "n.d." [b] Converted from DAS signal in ref 13.

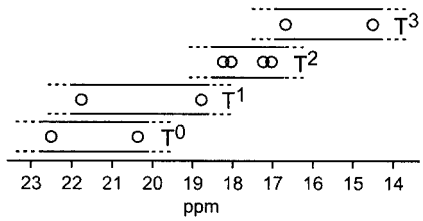

Figure 6. Schematic diagram of ^{11}B isotropic chemical shifts for compounds in this study. Open circles correspond to the compounds listed in Table 1; observed ranges of δ_{iso} for a given degree of connectivity are indicated by open-ended boxes.

MAS NMR data agree with a wide-line NMR study of triclinic magnesium pyroborate which found $C_Q = 2.81$ MHz and $\eta = 0.47$.[5] Despite peak overlap, the clearly identifiable singularities for magnesium orthoborate enabled the NMR parameters to be determined for this additional phase (Figure 4). No NMR data appear to have been published for this material. A ^{11}B wide-line NMR measurement of lanthanum orthoborate yielded a quadrupolar interaction with $C_Q = 2.74 \pm 0.05$ MHz (η was assumed to be zero).[37] Notwithstanding that subsequent developments in theory and instrumentation have cast doubt on the accuracy of this early value,[38] the C_Q obtained here is not unreasonable given the experimental uncertainties of both measurements.

^{11}B MAS NMR data for crystalline sodium metaborate and sodium pyroborate from a previous publication[21] are presented in Table 1. Quadrupole interaction parameters obtained in this study also agree with those previously determined by ^{11}B wide-line NMR.[5,39]

Discussion

The isotropic chemical shifts reported here exhibit a general trend toward higher δ_{iso} (i.e., greater deshielding) with the replacement of bridging oxygens by nonbridging oxygens. The existence of a given three-coordinate boron in a ring appears to have an additional deshielding effect for a given degree of connectivity (e.g., T^3 and T^2). The smallest δ_{iso} within this series belongs to B_2O_3 (Table 1, Figure 6), the crystal structure of which consists of spiraling T^3 chains.[40−42] Cesium enneaborate consists of two types of rings, boroxol rings and "triborate" rings possessing two three-coordinate borons (T^3(ring)) and one tetrahedral boron center.[18] Although the chemical shifts are not precisely determined for each of these species, they lie within a fairly narrow range of 16.5 to 16.9 ppm. In order of increasing chemical shift, the next two compounds are calcium metaborate and lithium metaborate, both containing T^2 chains.[43,44] Just to higher frequency of these systems lies sodium metaborate, which contains boroxol rings comprising T^2 units.[45] Potassium metaborate is also found in this region, if the DAS shift measured by Youngman and Zwanziger[46] is converted to the true δ_{iso} using quadrupolar parameters imported from the isomorphous sodium metaborate. Higher in frequency are found the sodium and magnesium pyroborates, involving the B_2O_5 dimer with T^1 units.[47] Among the largest chemical shifts observed in the series are those of the isolated T^0 groups in lanthanum orthoborate and magnesium orthoborate. The former is thought to have the aragonite structure[25] and the latter is isomorphous with cobalt orthoborate.[24] Although some overlap in these shifts is present, the general trend observed for this collection of compounds can be approximated as follows:

$$\delta_{iso}(T^0) \geq \delta_{iso}(T^1) > \delta_{iso}(T^2(\text{ring})) > \delta_{iso}(T^2) \geq \delta_{iso}(T^3(\text{ring})) > \delta_{iso}(T^3).$$

Similar correlations have been reported for other nuclear chemical shifts, with extensive experimental and theoretical work published on ^{29}Si and ^{31}P shielding. For four-coordinate silicon units in silicates, deshielding of δ_{iso} by approximately 10 ppm for every bridging oxygen replaced by a nonbridging oxygen is common,[48] thus leading to somewhat overlapping ranges for Q^n ($n = 0-4$) species,[49−51] as proposed here for T^n ($n = 0-3$). In phosphates, ^{31}P isotropic shifts are generally understood to follow the same pattern, with deshielding at four-coordinate phosphorus increasing as the network becomes depolymerized, Q^n ($n = 0-3$).[52,53] Again, secondary effects on the shifts such as the nature and number of charge-balancing cations are observed to produce significant overlap in these ranges, particularly those possessing the most nonbridging oxygens (i.e., Q^0 and Q^1).

(37) Bray, P. J.; Edwards, J. O.; O'Keefe, J. G.; Ross, V. F.; Tatsuzaki, I. *J. Chem. Phys.* **1961**, *35*, 435−442.
(38) Kriz, H. M.; Bray, P. J. *J. Magn. Reson.* **1971**, *4*, 69−75.
(39) Baugher, J. F.; Kriz, H. M.; Taylor, P. C.; Bray, P. J. *J. Magn. Reson.* **1970**, *3*, 415−426.
(40) Strong, S. L.; Kaplow, R. *Acta Crystallogr.* **1968**, *B24*, 1032−1036.
(41) Gurr, G. E.; Montgomery, P. W.; Knutson, C. D.; Gorres, B. T. *Acta Crystallogr.* **1970**, *B26*, 906−915.
(42) Strong, S. L.; Wells, A. F.; Kaplow, R. *Acta Crystallogr.* **1971**, *B27*, 1662−1663.
(43) Marezio, M.; Plettinger, H. A.; Zachariasen, W. H. *Acta Crystallogr.* **1963**, *16*, 390−392.
(44) Zachariasen, W. H. *Acta Crystallogr.* **1964**, *17*, 749−751.
(45) Marezio, M.; Plettinger, H. A.; Zachariasen, W. H. *Acta Crystallogr.* **1963**, *16*, 594−595.
(46) Youngman, R. E.; Zwanziger, J. W. *J. Am. Chem. Soc.* **1995**, *117*, 1397−1402.
(47) König, H.; Hoppe, R.; Jansen, M. *Z. Anorg. Allg. Chem.* **1979**, *449*, 91−101.
(48) Stebbins, J. F. In *Handbook of Physical Constants*; Ahrens, T. J., Ed.; American Geophysical Union: Washington, DC, 1995; Vol. 2, pp 303−332.
(49) Lippmaa, E.; Mägi, M.; Samoson, A.; Engelhardt, G.; Grimmer, A. R. *J. Am. Chem. Soc.* **1980**, *102*, 4889−4893.
(50) Smith, K. A.; Kirkpatrick, R. J.; Oldfield, E.; Henderson, D. M. *Am. Mineral.* **1983**, *68*, 1206−1215.
(51) Mägi, M.; Lippmaa, E.; Samoson, A.; Engelhardt, G.; Grimmer, A. R. *J. Phys. Chem.* **1984**, *88*, 1518−1522.

For nuclei with quadrupole moments, chemical shielding is less well understood, in part because the quadrupolar interaction often makes it difficult to obtain reliable shielding data in solids. Considerable effort has been expended to understand structural effects in ^{27}Al isotropic chemical shifts. While early NMR studies of aluminosilicate solutions suggested that analogous ^{27}Al shielding effects with condensation were operative,[54] these trends were not borne out in subsequent studies of solids.[55,56] The authors concluded that other effects were more important in these systems, and that the quadrupole coupling tensor was more sensitive to polymerization effects. A survey of ^{27}Al isotropic chemical shifts reveals that while Q^0 and Q^1 isotropic chemical shifts tend to be higher than those of fully polymerized $AlO_{4/2}$ groups in analogous systems,[48] there are many counterexamples which nullify the predictive power of this scheme.

Extensive theoretical efforts directed toward understanding the physical basis for measured chemical shifts have provided useful insights. Semiempirical[57] and ab initio[58,59] quantum chemical calculations have been used to rationalize observed correlations between δ_{iso} and a variety of structural and electronic parameters.[60] However attractive, simple correlations between isotropic chemical shift and local geometrical descriptors, such as average bond length r or average interbond angle, have been little more than suggestive in most cases of practical interest. This holds true in the present study, where although r_{BO} tends to be shorter for nonbridging oxygens than for bridging oxygens in T^1 and T^2 groups, the T^0 and T^3 units examined have r_{BO} for *both* bridging and nonbridging bonds ranging from about 1.23 to 1.44 Å. Moreover, the average bond length bears no obvious relation to either the degree of connectivity or the values of δ_{iso}. Similar commentary applies to the O−B−O and B−O−B angles.

Somewhat more useful appears to be an approach that accounts for longer range effects by tabulating the sum of all cation−oxygen bond strengths surrounding a given three-coordinate boron. Originally developed by Pauling to explain bond lengths in ionic crystals,[61] the concept of bond valence has become a useful empirical tool applicable to a wide variety of chemical bonding types.[62] Here, the procedure of Brese and O'Keeffe[63] is used in defining the valence v between two atoms as $\exp[(R - r)/b]$, where the parameter b is 0.37.[64] The *bond valence parameter R*, nominally the length of a single bond between the designated atoms, has been determined from a large number of crystal structures for many pairs of atoms, and is particularly well-established in oxides.[63] For a given oxygen, the total bond valence involves the sum of v to all cations within a specified radius. Hence, the sum over all three oxygens coordinated to boron provides an indirect measure of the influence of the next-nearest neighbors on the electronic environment at the ^{11}B nucleus being monitored by NMR.

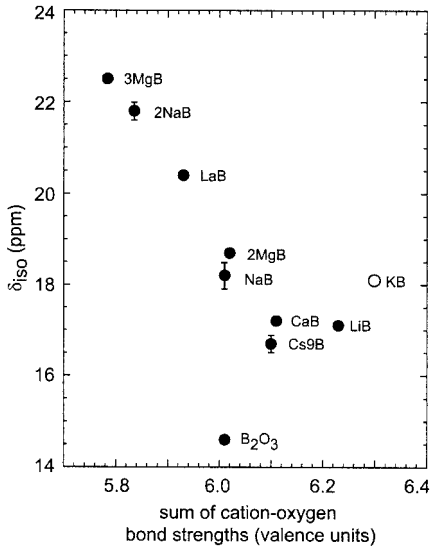

Figure 7. Relation of ^{11}B isotropic chemical shifts and the sum of cation-oxygen bond strengths for binary borates. Uncertainties in the shifts are within the bounds of the mark, except where indicated. The data point for KB is from ref 13.

Figure 7 depicts δ_{iso} plotted as a function of the bond strength sums. A roughly linear negative correlation is observed. This trend was first noted for $\delta_{iso}(^{29}Si)$ in silicates.[50] Figure 7 also suggests that the fundamental determinant of chemical shift is not the degree of network connectivity, but involves electronic effects which, in turn, are dependent on longer range atomic structure. If so, the utility of δ_{iso} in determining boron speciation in unknown materials, crystalline or amorphous, depends on the extent to which the number of bridging oxygens influences the pertinent electronic properties, and whether reasonable assumptions can be brought to bear on this ambiguity. Two apparent exceptions to the putative linearity are potassium metaborate and crystalline B_2O_3. Although an assumption about the quadrupolar coupling parameter has been made to obtain the true isotropic chemical shift for KB from the DAS signal of Youngman and Zwanziger,[46] this is unlikely to be the source of the anomaly, since the sum of the cation-oxygen bond strengths is unusually large, as previously noted.[65,66] The other data point that does not conform to the proposed relation is that of B_2O_3. While the reason for this is unclear, the wide range of r_{BO} in this compound (1.33−1.40 Å) have been linked to its lying well off the calculated bond order−bond length curve.[66] Lacking a comprehensive quantum mechanical treatment of these materials, the bond valence method appears to provide a means to evaluating the electronic environment at the nucleus of interest.

A variety of crystalline binary borates have been studied by ^{11}B MAS NMR to gain information about chemical shifts. In one of the first such studies,[67] Turner et al. made several comments regarding chemical shifts in borates and borosilicates at $B_0 = 11.7$ T. They suggested that the presence of Si in the next-nearest neighbor position increases shielding for both three- and four-coordinated boron, a supposition that has been tested in studies of various borosilicate glasses.[6,8,10,11,68−70] They hypothesized further that depolymerization would result in

(52) Kirkpatrick, R. J.; Brow, R. K. *Solid State Nucl. Magn. Reson.* **1995**, *5*, 9−21.
(53) Brow, R. K.; Kirkpatrick, R. J.; Turner, G. L. *J. Non-Cryst. Solids* **1990**, *116*, 39−45.
(54) Müller, D.; Hoebbel, D.; Gessner, W. *Chem. Phys. Lett.* **1981**, *84*, 25−29.
(55) Müller, D.; Gessner, W.; Samoson, A.; Lippmaa, E.; Scheler, G. *J. Chem. Soc. Dalton Trans.* **1986**, 1277−1281.
(56) Lippmaa, E.; Samoson, A.; Mägi, M. *J. Am. Chem. Soc.* **1986**, *108*, 1730−1735.
(57) Wolff, R.; Radeglia, R.; Vogel, C. *J. Phys. Chem. Solids* **1990**, *51*, 123−128.
(58) Wolff, R.; Radeglia, R.; Sauer, J. *THEOCHEM* **1986**, *139*, 113−124.
(59) Wolff, R.; Radeglia, R.; Vogel, C.; Sauer, J. *THEOCHEM* **1989**, *183*, 223−232.
(60) Engelhardt, G. *Stud. Surf. Sci. Catal.* **1989**, *52*, 151−162.
(61) Pauling, L. *J. Am. Chem. Soc.* **1929**, *51*, 1010−1026.
(62) O'Keeffe, M.; Brese, N. E. *J. Am. Chem. Soc.* **1991**, *113*, 3226−3229.
(63) Brese, N. E.; O'Keeffe, M. *Acta Crystallogr.* **1991**, *B47*, 192−197.
(64) Brown, I. D.; Altermatt, D. *Acta Crystallogr.* **1985**, *B41*, 244−247.
(65) Zachariasen, W. H. *J. Chem. Phys.* **1937**, *5*, 919−922.
(66) Schneider, W.; Carpenter, G. B. *Acta Crystallogr.* **1970**, *B26*, 1189−1191.
(67) Turner, G. L.; Smith, K. A.; Kirkpatrick, R. J.; Oldfield, E. *J. Magn. Reson.* **1986**, *67*, 544−550.

increased shielding at three-coordinate boron sites, concluding, however, that further work was needed to establish next-nearest neighbor effects.[67] Müller et al.[9] published ^{11}B MAS NMR results from which they concluded that within the uncertainty of their methods (±2 ppm), δ_{iso} is insensitive to structural influences other than coordination number, and hence can provide no detailed characterization of the structural units. The measurements on which this conclusion was based, however, were subject to several limitations. Principally, four- and three-coordinate boron signals overlap completely at 9.4 T, thus necessitating line shape fitting and increasing the uncertainty in chemical shift and quadrupole coupling constants. Moreover, because the influence of the quadrupolar interaction is larger with respect to the Zeeman interaction at lower fields, the second-order broadening and quadrupolar shift will be more significant, and the uncertainty in accounting for this shift will be greater than at higher fields. For example, the difference between Müller et al. and Turner et al.'s T^2 shift in potassium pentaborate is 1.9 ppm. Homonuclear dipolar broadening can be also significant for ^{11}B, with its natural abundance of 80%. In the present work, line shape singularities were observed to sharpen with increasing spinning speed up to about 15 kHz. In earlier works, spinning speeds were restricted to 5−6 kHz, insufficient to overcome dipolar broadening and therefore blurring some features of the line shape and adding uncertainty to the inferred NMR parameters. An additional consideration is that nearly all the compounds in the work of Müller et al. were hydrates, and the "nonbridging oxygens" are generally hydroxyl groups. Conclusions derived from this data set may not be directly applicable to anhydrous borates.

The trend reported in the present work is consistent with ^{11}B MAS NMR data on a series of sodium aluminoborate glasses.[71] Using NMR data collected at two magnetic fields, Züchner et al. fit the severely overlapping powder patterns corresponding to T^3, T^2, and T^1 groups to obtain relative populations and NMR parameters. Whereas four-coordinate boron chemical shifts are observed to increase smoothly on addition of alkali modifier, the three-coordinate boron groups have essentially discrete regions: T^3 (17.3−18.4 ppm), T^2 (19.0−19.8 ppm), and T^1 (19.6 and 20.0 ppm). Despite a fairly large measurement uncertainty (± 0.6 ppm) and anomalously small quadrupolar asymmetry parameters for the T^2 and T^1 groups, this report is supportive of the relationship proposed here on the basis of crystalline materials.

The significance of the ^{11}B isotropic chemical shift of crystalline B_2O_3 relates to the assignment of ^{11}B MAS NMR peaks in B_2O_3 glass (Figure 8) and the corresponding structural implications. The spectrum consists of two overlapping quadrupolar powder patterns which can be fitted to yield relative populations of 72:28, in agreement with previous estimates.[12,72−77]

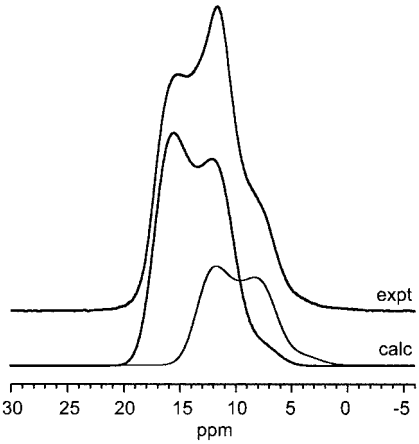

Figure 8. ^{11}B MAS NMR spectrum of B_2O_3 glass at 14.1 T, with individual calculated spectral components.

The more intense resonance possesses $\delta_{iso} = 18.3$ ppm and has traditionally been assigned to boron sites located in boroxol rings. The less intense peak has $\delta_{iso} = 14.5$ ppm and is attributed to those borons not in rings. The structure of crystalline B_2O_3 better resembles the latter.[41] At 14.6 ppm, the chemical shift for this phase is closer to that of the less populated boron site in the glass and is thus consistent with the conventional assignment. Also of interest in this regard are the three-coordinate ^{11}B chemical shifts in crystalline cesium enneaborate, the structure of which involves interlocking boroxol rings and triborate groups.[18] This low-alkali structure is the closest known crystalline analogue to the putative vitreous B_2O_3 structure.[78] The chemical shift of 16.7 ± 0.2 ppm is slightly lower than, but still supportive of the prevailing view for boroxol rings. This observation is also in agreement with theoretical calculations on model borate clusters, which suggest that borons in boroxol rings are deshielded relative to nonring borons.[79,80]

It is important to emphasize that the measured isotropic chemical shifts reflect the *average* shielding at a given nucleus, and thus distill to a single number dependencies in any of the three principal components of the second-rank tensorial property. More informative would be to compare the full shielding tensor (principal components and orientation of the principal axes in the molecular framework) with a high level quantum mechanical calculation of the electronic environment at a given nucleus. While this can be done in principle, experimental and theoretical limitations restrict this approach to select cases. For ^{11}B, the situation is further complicated by the quadrupolar interaction which perturbs the nuclear energy levels with respect to the pure shielding effects. While NMR spectra of nonspinning samples can yield shielding tensors in favorable circumstances, homonuclear dipolar interactions in these samples cause sufficient broadening to obscure the line shape characteristics required for reliable fits. Nonetheless, some information on the shielding tensor is available from a careful examination of the intensities of CT ssbs.

Figure 1b depicts the first spinning sideband to high frequency of the central peak of crystalline B_2O_3 along with spectral simulations including and not including anisotropic shielding. The relative intensities of the central and satellite transition spinning sidebands cannot be reproduced at 14.1 or 18.8 T without the introduction of a small, but significant degree of

(68) Villegas, M. A.; Sanz, J.; Navarro, J. M. F. *J. Non-Cryst. Solids* **1990**, *121*, 171−176.
(69) Bunker, B. C.; Tallant, D. R.; Kirkpatrick, R. J.; Turner, G. L. *Phys. Chem. Glasses* **1990**, *31*, 30−41.
(70) El-Damrawi, G.; Müller-Warmuth, W.; Doweidar, H.; Gohar, I. A. *J. Non-Cryst. Solids* **1992**, *146*, 137−144.
(71) Züchner, L.; Chan, J. C. C.; Müller-Warmuth, W.; Eckert., H. *J. Phys. Chem. B* **1998**, *102*, 4495−4506.
(72) Johnson, P. A. V.; Wright, A. C.; Sinclair, R. N. *J. Non-Cryst. Solids* **1982**, *50*, 281−311.
(73) Gravina, S. J.; Bray, P. J. *J. Magn. Reson.* **1990**, *89*, 515−521.
(74) Hannon, A. C.; Grimley, D. I.; Hulme, R. A.; Wright, A. C.; Sinclair, R. N. *J. Non-Cryst. Solids* **1994**, *177*, 299−316.
(75) Hwang, S.-J.; Fernandez, C.; Amoureux, J. P.; Cho, J.; Martin, S. W.; Pruski, M. *Solid State Nucl. Magn. Reson.* **1997**, *8*, 109−121.
(76) Joo, C.; Werner-Zwanziger, U.; Zwanziger, J. W. *J. Non-Cryst. Solids* **2000**, *261*, 282−286.
(77) Joo, C.; Werner-Zwanziger, U.; Zwanziger, J. W. *J. Non-Cryst. Solids* **2000**, *271*, 265−266.
(78) Wright, A. C.; Vedishcheva, N. M.; Shakhmatkin, B. A. In *Borate Glasses, Crystals and Melts*; Wright, A. C., Feller, S. A., Hannon, A. C., Eds.; Society of Glass Technology: Sheffield, UK, 1997; pp 80−87.
(79) Tossell, J. A. *J. Non-Cryst. Solids* **1995**, *183*, 307−314.
(80) Tossell, J. A. *J. Non-Cryst. Solids* **1997**, *215*, 326−243.

shielding anisotropy. In calculating these spectra, the nearly axially symmetric quadrupolar tensor ($\eta = 0.04$) was considered evidence for the presence of an approximate 3-fold rotation axis perpendicular to the BO_3 plane. Accordingly, the shielding tensor is constrained to axial symmetry ($\kappa = \pm 1$), with the unique component (i.e., the largest or the smallest) aligned with the largest component of the quadrupolar tensor. As described above, data at 14.1 and 18.8 T are best fit with a positive skew ($\kappa = +1$) and a shielding tensor spanning 15 ppm, indicating that the most shielded component is perpendicular to the BO_3 plane. The magnitude and orientation of the shielding tensor agrees with ab initio calculations on three-coordinate boron units in trimethyl borate.[81]

From an analogous treatment of Cs9B data at 14.1 and 18.8 T, the shielding tensor for the T^3(ring) sites is approximately 21 ppm, again with a positive skew. Here, multiple T^3 sites and a larger quadrupolar asymmetry parameter (0.2−0.3) cast greater uncertainty on these values, suggesting only that the shielding anisotropy is slightly larger than for B_2O_3. Several other analyses were made of the spinning sidebands in 14.1 T spectra for other compounds. For the T^0 group in lanthanum orthoborate, the axially symmetric quadrupolar tensor supports the assumption of coincident tensors, yielding a shielding anisotropy of $\Omega = 17 \pm 3$ ppm and $\kappa = +1$. In calcium metaborate (T^2) and magnesium pyroborate (T^1), the presence of nonbridging oxygens lowers the local symmetry, producing a nonzero quadrupolar asymmetry and almost certainly noncoincident, nonaxially symmetric shielding and quadrupolar tensors. With these unknowns it is not possible to report the shielding tensor components with confidence, however an exploration of several relevant parameters suggests that the shielding anisotropy is significantly larger in these compounds, spanning 35−40 ppm. These values are in agreement with ab initio calculations of T^2 groups in model clusters which indicate a skew of about 0, with a span ranging from 30 to 35 ppm.[82] These shielding data suggest that the small changes measured in δ_{iso} upon depolymerization result from larger changes in some or all of the tensor principal components, but are masked by opposite dependencies on structure. Thus, it would be most informative to measure the full tensors to gain a more comprehensive understanding of how shielding is correlated with structure.

In light of these suppositions, it is worthwhile to consider how applicable to studies of glass structure the observed correlation may be. Relationships between anisotropic shielding and structure have proven useful in nonspinning NMR studies of the spin-$^1/_2$ nuclides ^{29}Si and ^{31}P. The ^{29}Si shielding tensors in silicate tetrahedra with 0−4 nonbridging oxygens progress from isotropic to anisotropic ($\kappa = +1$) to anisotropic ($\kappa \approx 0$) to anisotropic ($\kappa = -1$) to isotropic, thus permitting structural conclusions and species quantification to be derived from appropriate experiments.[83,84] Similarly, phosphate tetrahedra exhibit the following behavior for 1 to 4 nonbridging oxygens: anisotropic ($\kappa = +1$), anisotropic ($\kappa \approx 0$), anisotropic ($\kappa = -1$), and isotropic.[85] For nuclei with quadrupolar interactions, the interplay between quadrupolar and shielding interactions often obscures information about both, especially in amorphous systems. However, sufficient ^{51}V ($S = ^7/_2$) shielding data on crystalline vanadates facilitated the use of ^{51}V NMR in the study of vanadium−niobium catalysts,[86] where it was concluded that the anisotropic shielding was a better structural indicator than δ_{iso}. At typical magnetic fields, however, this is a unique case in which the shielding interaction dominates the quadrupolar interaction. In general, the measurement of shielding tensors in the presence of quadrupolar interactions is not trivial. Preliminary ^{11}B NMR data at 18.8 T on borate glasses suggest that shielding anisotropy plays a role in the observed spinning sideband peak intensities (unpublished data). It is yet unclear whether this can be quantified with sufficient precision to have predictive power.

Conclusions

The detection of a subtle but significant relation between ^{11}B chemical shifts for three-coordinate boron and the degree of connectivity to other borate groups owes much to the use of relatively high magnetic fields of 14.1 and 18.8 T. Mainly due to the reduced influence of the quadrupolar interaction and enhanced prominence of the shielding interaction in the spectra, greater precision in δ_{iso} may be obtained relative to previous studies at lower fields and spinning rates. These effects are also advantageous in studies of glasses, where both three- and four-coordinated boron species are generally present. Whereas much of the early ^{11}B NMR work on borates relied on tedious fitting schemes to estimate the relative contributions of these sites to the spectra, MAS NMR studies of such systems at fields greater than 11.7 T conveniently offer complete resolution of the trigonal and tetrahedral boron sites. A direct comparison of these NMR approaches is provided in ref 87.

The particular correlation proposed here, as well as the general utility of using high field ^{11}B MAS NMR, opens up many possibilities for structural investigations of borate glasses. For example, using this approach to study high alkali binary borates or borosilicates may obviate the need to invoke assumptions about the degree of BO_3 polymerization in the development of structural models. Applications to mixed alkali glasses,[88,89] borosilicate,[90,91] aluminoborate,[92] and "invert glasses", where extensive depolymerization is expected, can be envisioned.

Acknowledgment. We are grateful to Prof. J. Puglisi for access to the Inova 800 at the Stanford Magnetic Resonance Laboratory, and to Dr. Corey Liu for excellent technical support. Dr. R. A. Smith (U. S. Borax) is acknowledged for providing the crystalline sample of B_2O_3. Dr. Peidong Zhao synthesized the sodium pyroborate sample. Helpful discussions with Dr. S. Sen (Corning, Inc.) regarding synthetic methodology are acknowledged. S.K. thanks the Natural Sciences and Engineering Research Council (NSERC) of Canada for a postdoctoral fellowship. This research is supported by the U.S. National Science Foundation (NSF) Grant DMR 9802072.

IC010305U

(81) Bryce, D. L.; Wasylishen, R. E.; Gee, M. *J. Phys. Chem. A* **2001**, *105*, 3633−3640.
(82) Tossell, J. A.; Sasaki, S. Personal communication, 2001.
(83) Zhang, P.; Grandinetti, P. J.; Stebbins, J. F. *J. Phys. Chem. B* **1997**, *101*, 4004−4008.
(84) Stebbins, J. F. *Nature* **1987**, *330*, 465−467.
(85) Eckert, H. In *NMR: Basic Principles and Progress*; Blümich, B., Ed.; Springer-Verlag: New York, 1994; Vol. 33, pp 125−198.
(86) Smits, R. H. H.; Seshan, K.; Ross, J. R. H.; Kentgens, A. P. M. *J. Phys. Chem.* **1995**, *99*, 9169−9175.
(87) Berryman, J. R.; Feller, S. A.; Affatigato, M.; Kodama, M.; Meyer, B. M.; Martin, S. W.; Borsa, F.; Kroeker, S. *J. Non-Cryst. Solids* **2001**. In press.
(88) Zhong, J.; Bray, P. J. *J. Non-Cryst. Solids* **1989**, *111*, 67−76.
(89) Ratai, E.; Janssen, M.; Eckert, H. *Solid State Ionics* **1998**, *105*, 25−37.
(90) Yun, Y. H.; Bray, P. J. *J. Non-Cryst. Solids* **1981**, *44*, 227−237.
(91) Dell, W. J.; Bray, P. J.; Xiao, S. Z. *J. Non-Cryst. Solids* **1983**, *58*, 1−16.
(92) Zhong, J.; Bray, P. J. *J. Non-Cryst. Solids* **1986**, *84*, 17−24.
(93) Fang, S. *Z. Kristallogr.* **1938**, *99*, 1−8.